J. Fluid Mech. (1971), *vol.* 46, *part* 3, *pp.* 569–576
Printed in Great Britain

Viscous tails in Hele-Shaw flow

By C. J. WOOD
Department of Engineering Science, University of Oxford

(Received 6 August 1970)

An experiment has been performed, using pulsed dye injection on an aerofoil in a Hele-Shaw cell. The purpose was to observe the form of the trailing-edge flow when the Reynolds number was high enough to permit separation and the initiation of a Kutta condition. The experiment provides a successful confirmation of the existence of a 'viscous tail' as predicted by Buckmaster (1970) although there is an unexplained quantitative discrepancy.

Introduction

In a recent paper Buckmaster (1970) pointed out that in Hele-Shaw flow an aerofoil must begin to generate circulation and lift as soon as the Reynolds number becomes large enough for separation to occur at the trailing edge. Experiments by Riegels (1938) were cited to show that this should take place when the Reynolds number, modified to take account both of the aerofoil chord c† and the plate spacing $2h$†, and defined by

$$\Lambda = 2Uh^2/\nu c \tag{1}$$

became of order unity.

By setting up averaged equations of motion in terms of the peak value of the parabolic viscous velocity distribution between the plates, Buckmaster was able to predict that after the onset of separation the bound circulation should be matched by a corresponding trailing vorticity distribution in the form of an exponentially decaying shear layer in the wake; the strength $\gamma(s)$ of this shear layer at dimensionless distance s chord lengths from the trailing edge was given by

$$\gamma(s)/U = (2N\Gamma/Uc)\exp(-2Ns), \tag{2}$$

where $N = 15/4\Lambda$, and Γ is the bound circulation.

The proximity of this trailing circulation to the aerofoil produces a downwash at the surface, so reducing the effective incidence and the bound circulation to a value given by Buckmaster for a flat plate at incidence α as

$$2\Gamma/Uc = 2\pi\alpha\bigg/\left\{1 + 2N\int_0^\infty \exp-(2Ns)\left[\left(\frac{s+1}{s}\right)^{\frac{1}{2}} - 1\right]ds\right\}. \tag{3}$$

† The use of the half-chord and half spacing as reference dimensions is not stated explicitly by Buckmaster but is deduced from the limits applied to the integrals in his equations (5) and (18). The equations quoted here are modified to take account of this difference in notation.

Buckmaster reported that a brief and unsuccessful attempt had been made to observe this phenomenon in a Hele-Shaw cell at the Oxford University Engineering Laboratory. It is the purpose of the present paper to describe some subsequent, more careful experiments which were successful.

Experimental procedure

The Hele-Shaw flow was established, not in a conventional high-pressure cell but in a commercially produced 0·9 × 0·6 m 'Sandover table'. In this apparatus, water flows under a very small head between a pair of horizontal glass plates spaced by strips of 3·2 mm Perspex at the streamline edges.

The extreme sensitivity of Hele-Shaw flow to variations in plate spacing was used during initial calibration tests with no model to check that the glass plates were sufficiently flat and parallel. It was found that provided the spacer strips were cleaned carefully to remove any particles of dirt, a series of dye lines would invariably flow straight and parallel across the whole table.

The model, made also of 3·2 mm black Perspex was a 10 % thick symmetrical aerofoil of 153 mm chord and having a sharp trailing edge of 12° total angle. The flow was made visible by injecting blue dye (13 parts Sulphan Blue to 1 part Trypan Blue at a concentration of about 1 g/l) through suitably placed hypodermic tubes. One of these tubes passed through a hole in one of the cover plates and into the model itself, thus forming a convenient pivot for incidence setting. Inside the model, the dye passed along a chordwise manifold to reach two identical drillings which allowed it to flow out symmetrically on either surface of the aerofoil just upstream of the trailing edge. These holes were enlarged to 1·5 mm diameter at exit in order to pass fairly large quantities of dye at very low ejection velocities.

In order to observe the viscous tail, it was necessary to detect a difference in velocity on opposite sides of the wake. Normal continuous dye filaments cannot fulfil this purpose of course, so the two trailing-edge dye filaments were interrupted at a regular frequency by incorporating an interruptor valve in the supply tube. This simple rotary valve was constructed by fitting a P.T.F.E. sleeve round a 3·2 mm diameter polished steel spindle and drilling a common 1·2 mm hole diametrically through both. The dye supply was passed through this hole so that, as the spindle was rotated in the fixed sleeve by a small electric motor, the flow was allowed to pass in a brief pulse, twice during each revolution.

After considerable experimentation with the motor speed, the pressure in the dye supply reservoir and the concentration of the dye solution, the equipment was adjusted successfully to produce regular streams of coherent dye pulses simultaneously and symmetrically from both sides of the model. The maximum useful frequency was 1·6 pulses/s. Provided that this was not exceeded, the dye pulses remained clearly distinguishable for more than a chord length downstream of the trailing edge (figure 1, plate 1).

It was only during the final analysis of the experimental results that a fault was revealed in the construction of the interruptor valve. Systematic errors in the velocity calculations were traced to the fact that successive dye pulses were spaced by time intervals which were alternately slightly above and slightly below the average value measured by stopwatch. This occurred because the diametral hole in the valve was very slightly off-centre. However, as will be seen later, the error was eliminated by careful averaging of the results and it was not thought necessary to repeat the experiment with a new valve.

When finally set up to give satisfactory photographs, the undisturbed stream velocity was 0·424 m/s, measured by timing the travel of a dye marker over a measured distance well away from the model. At a water temperature of 18·7 °C and with the dimensions already specified, this yielded a modified Reynolds number Λ of 1·30 and correspondingly $N = 2{\cdot}88$.

The flow was photographed on half-plate 400 ASA film at *f*. 16 with the aid of an electronic flash placed beneath the flow table and shining directly up towards the camera through a translucent white Perspex diffusion screen. A grid of 1 in. (2·54 cm) squares inscribed on the lower glass plate gave a record of the magnification.

Results and discussion

Incidence values from 0 to 25° by 5° increments were used, and similarly from $-2{\cdot}5°$–$2{\cdot}75°$. Figure 1 (plate 1) shows the flow at 10° incidence, and if the dye pulses are paired correctly, counting from the right, it is immediately obvious that there is a velocity difference between the upper and lower sides of the wake and that this difference becomes less pronounced with increasing distance. Thus the photographs provide a direct qualitative confirmation of the existence of viscous tails at $\Lambda = 1{\cdot}30$.

Having obtained a convincing set of photographs, it was decided to measure them in order to investigate whether there was any quantitative agreement between the observed flow and the predictions of Buckmaster.

Neglecting the downwash angle, the photographs were measured to determine the streamwise position reached by the front of each dye pulse relative to the trailing edge. These displacements were first plotted against the age of the pulse, and since the resulting curves were smooth with no great curvature it was decided to estimate the local velocities directly from these displacement measurements by means of the linear approximation

$$u(x) = (x_n - x_{n+1})/\tau,$$

where $x = \frac{1}{2}(x_n + x_{n+1})$ and τ is the time interval between successive pulses.

Although the distribution of dye across the gap between the plates is not known, it can be assumed with confidence that some dye will remain on the central plane of symmetry. This portion travels faster than the rest in the parabolic viscous velocity distribution so that the foremost edge of the dye pulse always gives a true indication of the peak velocity. This is the velocity defined and used by Buckmaster.

Disappointingly, these velocities did not lie on smooth curves but were in all cases staggered in an alternating pattern as shown in figure 2. The cause of this was the hitherto undetected fault in the dye interruptor valve already described.

Fortunately it was easy to eliminate this error by first drawing curves through the odd points and the even points separately and then drawing the final curve as the average of the two. This procedure was adopted for all the velocity estimates on both top and bottom sides of the wake.

Photograph	Incidence (deg)	(γ/U) (0·1)	(γ/U) (0·6)	a	γ_0/U	γ_0/Ua
1	0	0	0	.	0	0
2	5	0·311	0·105	2·17	0·386	0·178
3†	10	0·483	0·090	3·36	0·675	0·201
4	15	0·585	0·190	2·25	0·731	0·325
5	20	0·721	0·224	2·34	0·911	0·389
6	25	0·903	0·355	1·87	1·090	0·583
7	−2·5	−0·105	−0·049	1·52	−0·122	−0·081
8	−7·5	−0·288	−0·098	2·16	−0·358	−0·166
9	−12·5	−0·478	−0·140	2·45	−0·610	−0·249
10	−17·5	−0·693	−0·246	2·07	−0·851	−0·412
11	−22·5	−0·860	−0·385	1·61	−1·010	−0·628
12	−27·5	−1·075	−0·425	1·85	−1·293	−0·700

† This case was used for illustration in figures 1–3.

TABLE 1. Tabulated experimental results

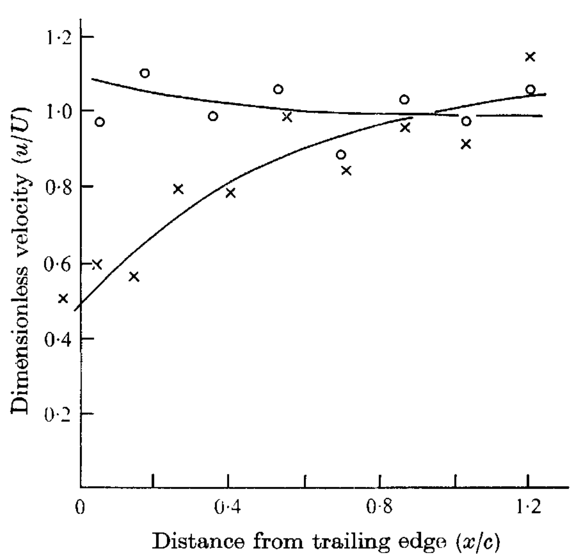

FIGURE 2. Velocity distributions beside the wake at 10° incidence (measured from figure 1). ○, upper side; ×, lower side.

For each incidence the upper and lower velocity curves were subtracted in order to find the vortex sheet strength $\gamma(x)$. The curve shown in figure 3 for 10° incidence is derived from figure 2 and corresponds to the photographs in figure 1. The results for all the other cases are tabulated in table 1.

Buckmaster (1970) has predicted that the vortex sheet should decay exponentially (see equation (2)). Therefore a curve of the form

$$\gamma(x)/U = \gamma_0/U \exp(-ax/c)$$

was fitted to the experimental results at two arbitrarily chosen points $x/c = 0{\cdot}1$ and $x/c = 0{\cdot}6$. The agreement was uniformly good throughout the incidence range although the exponential always had rather more curvature than the experimental line (figure 3). This type of discrepancy could well result from the rather crude nature of the velocity measurements. With the dye markers forming at a finite distance to the side of the wake streamline, the normal potential flow decay in the disturbance velocity would tend to lead to an underestimate of the shear layer strength, especially near the trailing edge.

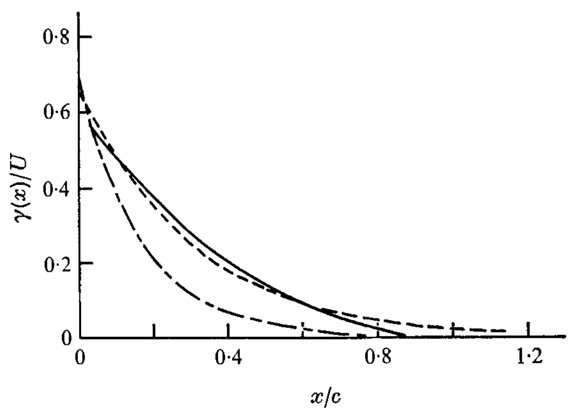

FIGURE 3. Vortex sheet strength at 10° incidence (velocity difference from figure 2). ——, experimental curve; ------, best exponential curve $\gamma(x)/U = 0{\cdot}675 \exp(-3{\cdot}36\, x/c)$; — — —, Buckmaster prediction (equation (2.3)) $\gamma(x)/U = 0{\cdot}697 \exp(-5{\cdot}72\, x/c)$.

It is also probable that the conditions of the experiment exceed the limits of validity of the linear assumption in Buckmaster's analysis. This assumption implies that the mean of the upper and lower wake velocities is equal to the undisturbed stream velocity, whereas figure 2 demonstrates that in the present experiments this is not so, particularly near the trailing edge.

A far more serious discrepancy, and one for which the author can as yet offer no explanation, is found in the numerical value of the decay exponent. As already stated, the Reynolds number of the present experiments corresponds to the value $N = 2{\cdot}88$. According to Buckmaster's analysis and allowing for differences in notation, this gives a theoretical exponent of 5·76 (see equation (2)) However, the value of the exponent a deduced from the present experiments is only 2·15 (table 1). This difference is nearly eight times as great as the r.m.s. deviation in the experimental results and clearly requires further investigation.

Leaving this difficulty for the moment we turn to one other interesting point of comparison between experiment and theory. This is the total circulation for which Buckmaster's prediction is quoted here in (3). For the present purpose, the integral was evaluated approximately for various values of N using a binomial expansion in terms of gamma functions. The convergence became poor for $N < 2$, nevertheless the form of the expression gives a clear indication of the limiting value when $N = 0$. This case corresponds to the potential flow circulation $\Gamma/Uc = \pi\alpha$. The solution is plotted in figure 4.

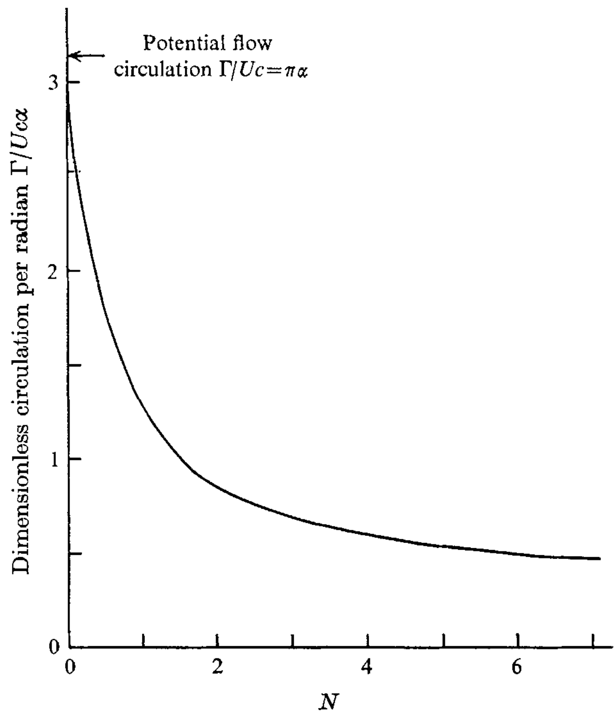

FIGURE 4. Approximate evaluation of equation (3).

To estimate the circulation in the present experiments, use is made of the fact that the bound circulation on the aerofoil has the same magnitude as the total circulation about the wake. This latter was estimated by integrating the exponential approximation to the experimental vortex sheet (equation (4)) to give

$$\Gamma/Uc = \gamma_0/Ua.$$

The result for each angle of incidence is shown in table 1 and is plotted against incidence in figure 5. These points are compared with both the potential flow line and the Buckmaster prediction for the present experimental value of N. Qualitatively, the predicted reduction in circulation is clearly demonstrated but again the quantitative agreement is poor. It is easy to demonstrate that this disagreement follows directly from the fundamental discrepancy in the decay exponent, and not from the subsequent downwash analysis leading to (3). If (3) is evaluated for $N = 1{\cdot}07$ corresponding to the mean experimental exponent ($a = 2{\cdot}15$) instead of for $N = 2{\cdot}88$, then the slope of the circulation line becomes $1{\cdot}21$ per radian instead of $0{\cdot}70$ and the agreement in figure 5 becomes quite good.

In considering possible explanations for this discrepancy it must be noted that

Buckmaster's potential flow analysis is linear and applies strictly to small inclinations of slender aerofoils. Unfortunately the accuracy of the present results in figure 5 is not sufficient to show whether the agreement improves at small incidence.

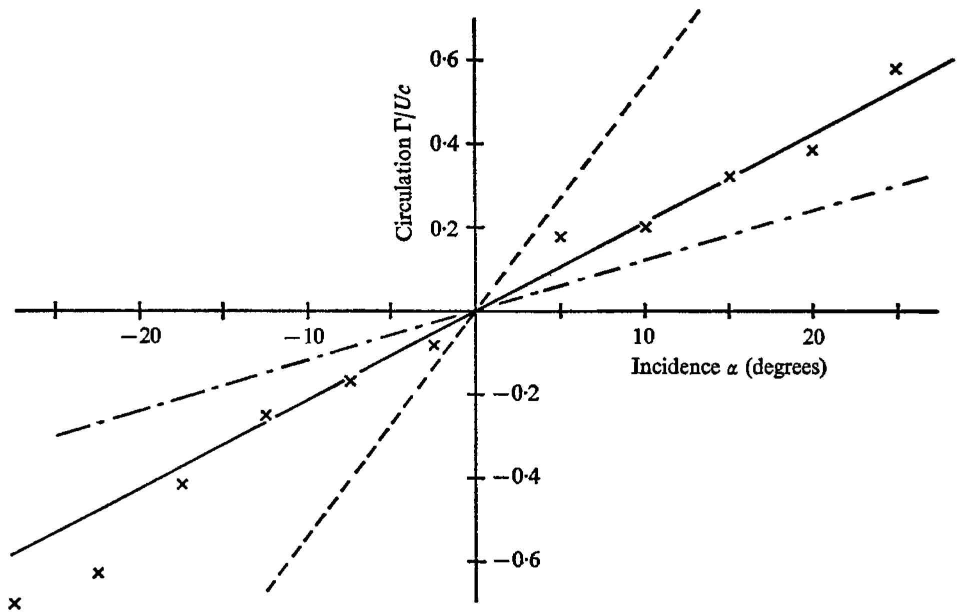

FIGURE 5. Variation of circulation with incidence. – – –, potential flow; – - –, equation (3), $N = 2{\cdot}88$; ——, equation (3), $N = 1{\cdot}07$; ×, experiment.

Apart from this, it is possible for an experimental error to arise if the wake where secondary effects still exist were to spread sufficiently to entrain the dye markers at some distance from the trailing edge. This would reduce the apparent local shear layer strength towards the downstream end of the wake and may possibly be the cause of the rather sharp final decay in the experimental results (figure 3). However, this still does not explain why the overall experimental decay rate is significantly lower than predicted, and it would appear that a more sophisticated investigation is necessary.

Conclusion

It has been verified by a simple quantitative flow visualization experiment that in limiting Hele-Shaw flow between plates $2h$ apart at a modified Reynolds number

$$2Uh^2/\nu c = 1{\cdot}3$$

there exists a viscous tail behind a lifting aerofoil. This takes the form of an exponentially decaying shear-layer wake.

The presence of the viscous tail causes a downwash on the aerofoil, reducing the bound circulation below the potential flow value by an amount which can be predicted accurately from simple potential flow considerations. However, the decay rate of the experimental shear layer did not agree with a prediction by Buckmaster. The reason for this discrepancy has yet to be explained.

The author wishes to thank Mr M. E. Byford, who persevered with the development of the dye injection technique until the required results could be obtained.

REFERENCES

Buckmaster, J. 1970 *J. Fluid Mech.* **41**, 523.
Riegels, F. 1938 *Z. angew. Math. Mech.* **18**, 95.

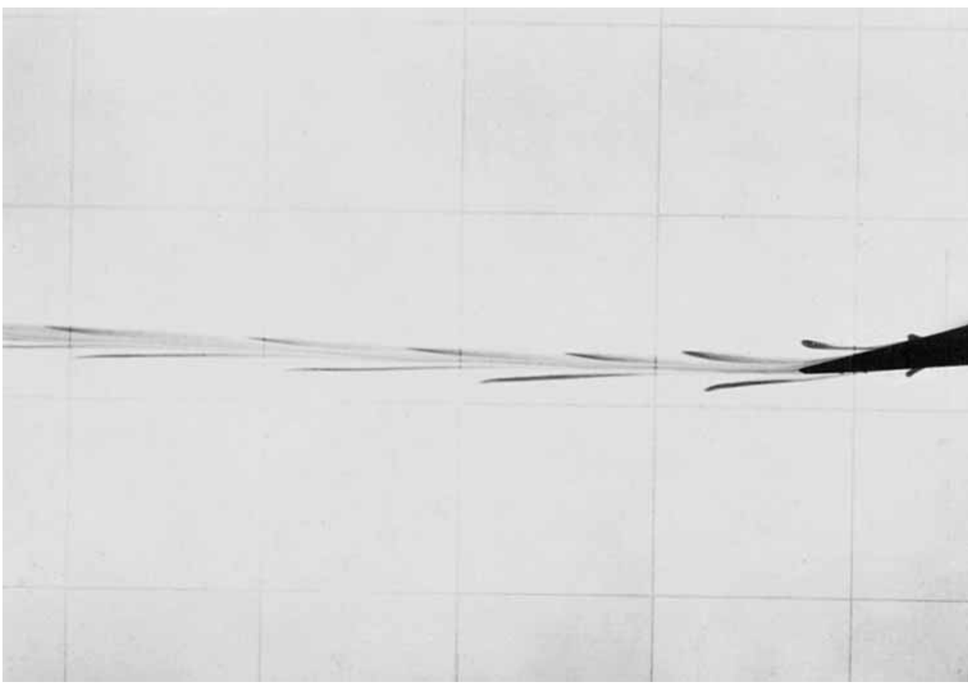

FIGURE 1. Wake at 10° incidence.